Desalination and Water Treatment
www.deswater.com

doi: 10.5004/dwt.2021.27770

238 (2021) 294–305
October

Removal of Congo red using the chlorinated Ca-Al layered double hydroxide produced from the desulfurization circulating wastewater

Xiuqin Kong*, Nini Zhang, Yiming Lian, Qianjun Tang

School of Petrochemical Engineering, Lanzhou University of Technology, Lanzhou 730050, Gansu, China, email: xqkong2@126.com (X.Q. Kong), Tel. 13893349788; emails: 914627791@qq.com (N.N. Zhang), 2506208735@qq.com (Y.M. Lian), 705197567@qq.com (Q.J. Tang)

Received 11 May 2021; Accepted 26 August 2021

ABSTRACT

The recycling and utilization of the solid precipitate produced by the treatment of the chlorine-containing desulfurization circulating wastewater using ultra-high lime with the aluminum process were studied. By means of X-ray diffraction, Fourier-transform infrared, scanning electron microscopy and volumetric adsorption analyzer, it was proved that the main composition of the precipitation was the chlorinated Ca-Al layered double hydroxide (CaAl-LDH-Cl). This precipitation was named waste-CaAl-LDH-Cl in this paper. It was used as an adsorbent to remove Congo red (CR). The research showed that waste-CaAl-LDH-Cl is an effective adsorbent for the removal of CR dye from the aqueous solutions. Adsorption of CR was found to increase with the increase of contact time, initial dye concentration and solution temperature. The adsorption of CR on waste-CaAl-LDH-Cl was favored at an acidic medium. The adsorption kinetics followed the pseudo-second-order model, whereas Langmuir adsorption isotherm fitted better to obtained data. The highest adsorption of 123.9 mg/g was recorded at 90 min and 313 K. $\Delta G°$ = –2.6757, –6.8761 and –12.7107 kJ/mol, $\Delta H°$ = 301.1145 kJ/mol, these data suggested that the adsorption process was spontaneous and endothermic. The adsorption mechanism included the electrostatic interaction, hydrogen bond and surface complexation. The results suggested that waste-CaAl-LDH-Cl is an efficient material for the removal of anionic organic pollutants from the wastewater.

Keywords: Layered double hydroxide (CaAl-LDH-Cl); Congo red; Adsorption

1. Introduction

Chloride ion is a typical corrosive ion, which destroys the metal passive film corrode metal pipes and other equipment after reaction with dissolved oxygen in water [1]. In addition, a high concentration of chloride ions also affects the quality of gypsum, the durability and quality of concrete, and even damages buildings. Besides, chloride ios have toxic effects on plant growth and can also severely pollute groundwater and drinking water [2]. Chloride ion is easily soluble in water but difficult to remove, therefore, it exists in high content in industrial wastewaters, such as wet flue gas desulfurization and denitrification wastewater [3], cooling circulating water [4], pickling wastewater and others [5].

The high concentration of chloride ions in some wastewaters will inhibit the growth of microorganisms, so these wastewaters cannot be direct. Currently, chlorine ion removal technologies mainly include chemical precipitation technology [6], ion exchange method [7], electrochemical technology [8,9], and other technologies [10]. Among them, the chemical precipitation method is suitable for the treatment of wastewaters with high concentrations of chloride, while ion exchange technology, electrochemical

* Corresponding author.

technology, membrane method and adsorption method are generally only applicable to wastewaters with low concentrations. In the chemical precipitation method, the ultra-high lime with the aluminum process is considered to be an economical and effective chloride removal technology. This treatment method is based on the addition of excess, which is to add excess calcium salt and aluminum salt into the solution to react with chloride ions. Under a certain reaction temperature and stirring speed, the precipitate of calcium aluminum layered double hydroxides (CaAl-LDH-Cl) is formed, which finally realizes the effective removal of chloride ions [11,12]. At present, there is much research on the treatment of high chloride wastewaters by ultra-high lime with the aluminum process. Fang et al. [3] carried out the research on the removal of chloride ions from the wet flue gas desulfurization and denitrification wastewater using Friedel's salt precipitation method. The two-stage Friedel's salt precipitation method was used to remove sulfate ion and chloride ion respectively, with the removal percentage of 98% and 85%, and it has a synergistic effect on other anions and heavy metal ions. Abdel-Wahab and Batchelor [13] explored the effects of pH value, temperature and reagent dosage on the chloride ion removal efficiency of the process treating recirculated cooling water. The results showed the optimum pH value is 12 ± 0.2, the reaction temperature should not exceed 40°C, and the optimum molar ratio of Ca^{2+} and Al^{3+} is 2.5.

The layered double hydroxide (LDH) is a versatile class of ionic clay consisting of the main layer with a positive charge and an intermediate layer with a negative charge. It has a general formula expressed as $[M^{2+}_{1-x}M^{3+}_{x}(OH)_2]^{x+}(A^{n-})_{x/n}\cdot mH_2O$ where M^{2+} represents the divalent metal cations such as Ni^{2+}, Cu^{2+}, and so forth, M^{3+} represents the trivalent metal cations such as Mn^{3+} and Al^{3+}, A^{n-} is the anion, and X is the molar ratio of the trivalent metal ion to total metal ions. LDH is favorable adsorbent material because of its excellent physical and textural characteristics [14,15]. Previous studies have also proved this point. Dao et al. [16] synthesized Ni-Fe LDH by hydrothermal method and the study showed that the Congo red (CR) removal capacity reached a maximum value of 244.87 mg/g at a concentration of 136.63 mg/L, pH of 5.94 and reaction time 233.84 min. Lafi et al. [17] synthesized Mg-Al LDH by co-precipitation method and the CR removal capacity reached a maximum value of 111.11 mg/g. Tolonen et al. [18] researched that the removal of sulfate from mine water by precipitation as ettringite (CaAl-SO_4-LDH) and the utilization of the precipitate as a sorbent for arsenate removal (q_m = 11.2 ± 4.7 mg/g). Wu et al. [19] studied the removal of phosphate using ettringite synthesized from industrial by-products. The removal capacity (q_e) for phosphate removal fluctuated in the range from 160 to 211 mg/g.

As mentioned above, both LDH synthesized by chemical method and ettringite synthesized from industrial by-products have related studies, but the treatment and disposal of waste calcium aluminum layered double hydroxides (waste-CaAl-LDH-Cl) produced from the desulfurization circulating wastewater (DCW) has not been reported. Therefore, this paper focuses on the recycling and utilization of waste-CaAl-LDH-Cl as an adsorbent of CR. Firstly, the waste-CaAl-LDH-Cl was obtained by the ultra-high lime with aluminum method from DCW. Secondly, the performance and mechanism of waste-CaAl-LDH-Cl as an adsorbent to adsorb CR were studied.

2. Materials and methods

2.1. Materials

All chemical reagents are analytically pure and directly used without any further purification. $Ca(OH)_2$, $NaAlO_2$ and CR were used in the experiments. The actual wastewater (the wet flue gas desulfurization circulating wastewater, DCW) was obtained from a power plant located in Henan Province, China. The wastewater quality parameters are shown in Table 1.

2.2. Preparation of waste-CaAl-LDH-Cl

The waste-CaAl-LDH-Cl was prepared by using the two-stage ultra-high lime with the aluminum process to treat the DCW. In the first stage, SO_4^{2-} was removed. The conditions are as follows: the molar ratio of $Ca(OH)_2$:$NaAlO_2$:SO_4^{2-} = 4:1:1, T = 27°C, t = 17 min, the stirring speed was 200 rpm, and the pH value remains unchanged. In the second stage, chloride ion was removed, with the molar ratio of $Ca(OH)_2$:$NaAlO_2$:Cl^- = 6:3:1, T < 40°C, t = 30 min, r = 300 rpm. The solid precipitation from the second stage was waste-CaAl-LDH-Cl that was collected, dried in a muffle furnace, ground and sieved through 100 mesh.

2.3. Congo red

Congo red (CR) is commonly used in the textile industry to give wool and silk red color with yellow fluorescence. The effluent containing CR is largely produced from textiles, printing, dyeing, paper and plastic industries, etc. Due to its good water-solubility and stability, CR is difficult to be degraded, causing potential harm to animals, plants, the human body and the environment. Therefore, it is important to remove CR from wastewater. Table 2 shows the characteristics of CR. The CR solution was prepared just before use.

2.4. Analytical methods

The waste-CaAl-LDH-Cl was characterized by scanning electron microscopy (SEM), X-ray diffraction (XRD), Fourier-transform infrared (FTIR) and volumetric adsorption analyzer. The SEM (JSM-6701F, Japan) was obtained at the voltage of 5 kV. The XRD (D/MAX-2400X, Japan) patterns were obtained with a diffractometer (4 kV, 100 mA), a scan range from 2° to 80° and a scan rate of 2°/min^{-1}. The FTIR spectra (Nicolet NEXQS670, USA) were measured on a spectrometer in the range of 4,000–400 cm. The specific surface area and the total pore volume were determined using a volumetric adsorption analyzer (Micromeritics ASAP 2020, USA). The specific surface area and pore size of the waste-CaAl-LDH-Cl were calculated by the Brunauer–Emmett–Teller (BET) and Barrett–Joyner–Halenda (BJH) method, respectively. Furthermore, the chloride concentration was determined by gel electrode (JENSPRIMA innoCon

Table 1
Wastewater quality parameters

Index	Desulfurization circulating wastewater (mg/L)
Chemical oxygen demand	666.4
SO_4^{2-}	2,104
Cl^-	1,565
pH	8.3

Table 2
Characteristics of Congo red

Molecular formula	$C_{32}H_{22}N_6Na_2O_6S_2$
Molecular weight (g/mol)	696.67
λ_{max} (nm)	498
Chemical class	Anionic
Chemical structure	Fig. 1
C.I. number	22120
C.I. name	Direct red 28

601, China) and the calcium concentration was determined by ethylenediamine tetraacetic acid titration.

2.5. Adsorption experiments

The waste-CaAl-LDH-Cl was used as an adsorbent to treat CR dye. The effects of initial CR concentration, contact time, solution temperature and solution pH on the CR uptake were investigated. All the batch experiments were carried out in a 250 mL flask. The waste-CaAl-LDH-Cl (0.4 g/L) was added to the CR solution and shaken for 90 min to achieve the adsorption equilibrium. After equilibrium, the samples were centrifuged at 6,000 rpm for 10 min, then the CR concentration in the supernatant was determined by a UV-Vis spectrophotometer (UV-5200, China) at the wavelength of 498nm. All experiments were carried out in three parallel experiments. The adsorption capacity of the adsorbent and the percentage of removal CR were calculated by Eqs. (1) and (2), respectively:

$$q_t = \frac{\left(c_0 - c_t\right) \times V}{m} \tag{1}$$

$$R = \frac{c_0 - c_e}{c_0} \times 100\% \tag{2}$$

where q_t is the adsorption capacity (mg/g) at any time, R is CR removal percentage (%), c_0 is the initial CR concentration (mg/L), c_t is the CR concentration at any time, c_e is the equilibrium concentration of CR, m is adsorbent mass (g) and V is the volume of the CR solution (L).

2.5.1. Effect of contact time and CR initial concentration

In order to study the effect of contact time and initial dye concentration on the CR uptake. The experimental conditions were as follows: C(CR) = 30, 40 and 50 mg/L, m(waste-CaAl-LDH-Cl) = 0.4 g/L, V = 100 mL, t = 90 min, T = 303 K, r = 200 rpm. In this case, the solution pH was kept original without any pH adjustment. Among them, C, m, V, t, T and r are the initial concentration of CR, the dosage of adsorbent, the volume of solution, the reaction time, temperature and the rotation speed of shaker, respectively.

2.5.2. Effect of solution temperature on CR adsorption

The effect of solution temperature on the CR adsorption process was examined by varying the adsorption temperature by adjusting the temperature of the gas bath shaker (Model THZ-82A, China). The experimental conditions were as follows: T = 303, 308 and 313 K, C(CR) = 50 mg/L, m(waste-CaAl-LDH-Cl) = 0.4 g/L, V = 100 mL, t = 90 min, r = 200 rpm. The solution pH was kept original without any pH adjustment.

2.5.3. Effect of solution pH on CR adsorption

The effect of solution pH on the CR adsorption process was studied by varying the initial pH of the solution. The initial pH of the CR solution was 7.91. The pH was adjusted using 0.1 M HNO_3 (HCl can affect the determination of Cl^-) and 0.1 M NaOH and was measured using a pH meter (Model PHS-3C, China). The experimental conditions were as follows: pH = 4, 6, 10 and 12, C(CR) = 50 mg/L, m(waste-CaAl-LDH-Cl) = 0.4 g/L, V = 100 mL, t = 90 min, T = 303 K, r = 200 rpm.

3. Results and discussion

3.1. Characterization

The BET surface area and pore characteristics were calculated according to the N_2 adsorption–desorption isotherm and pore size distribution of the waste-CaAl-LDH-Cl (Fig. 2a). The waste-CaAl-LDH-Cl had a surface area of

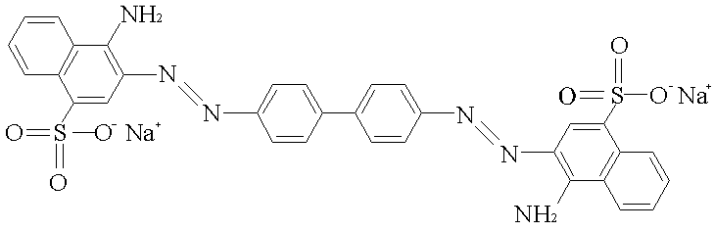

Fig. 1. Chemical structure of CR dye.

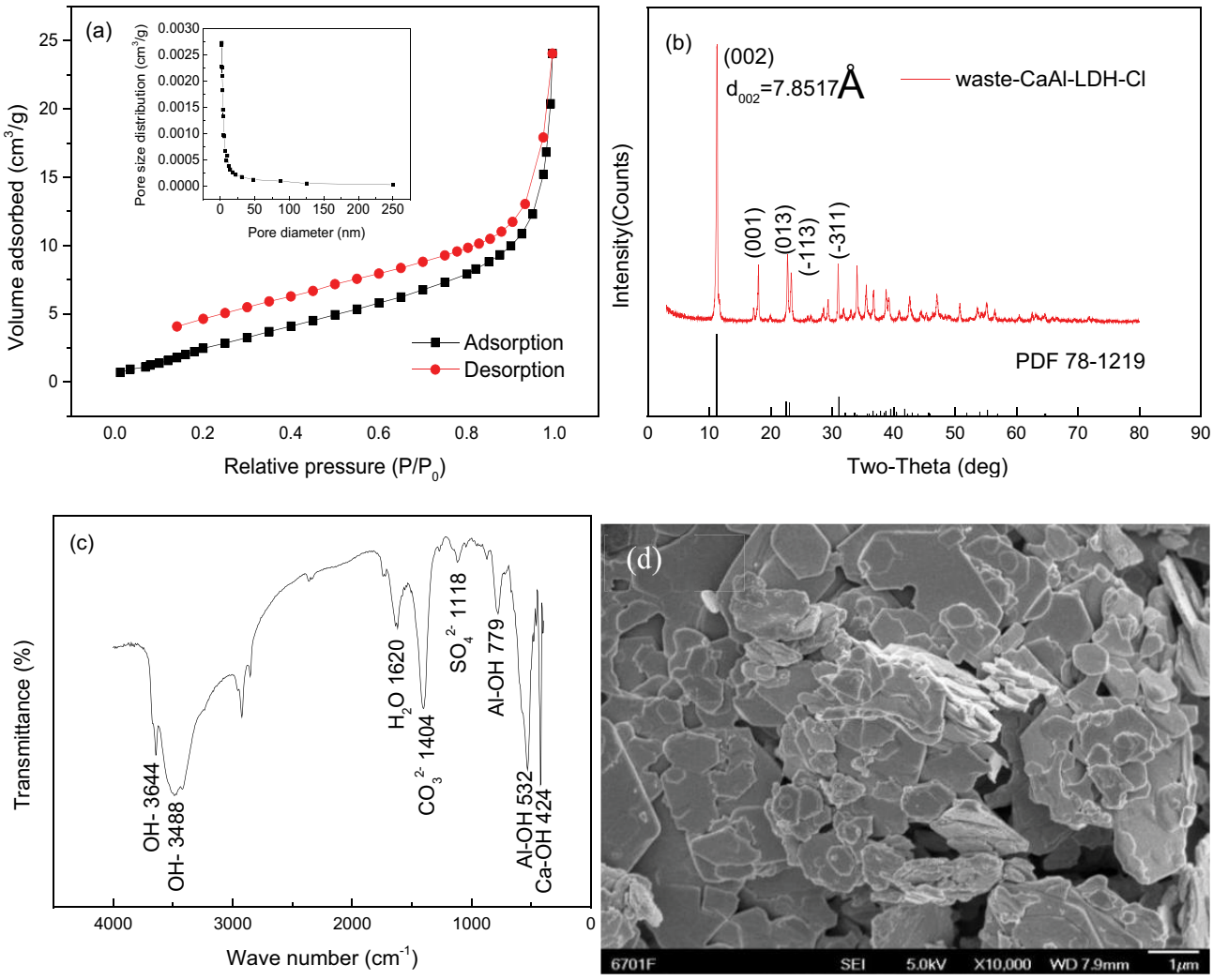

Fig. 2. (a) N_2 adsorption–desorption isotherms and pore size distribution curve, (b) XRD pattern, (c) FTIR spectrum and (d) SEM morphologies of waste-CaAl-LDH-Cl.

13.95 m^2/g, a total pore volume of 0.0235 cm^3/g, and an average pore diameter of 6.74 nm. Therefore, the above analyses resulted that waste-CaAl-LDH-Cl obtained from the DCW by ultra-high lime with the aluminum process was a mesoporous material. As a result, the waste-CaAl-LDH-Cl was completely feasible to be used as an adsorbent.

The crystal structures of the materials were characterized by XRD. From Fig. 2b, the XRD pattern of waste-CaAl-LDH-Cl showed characteristic diffraction peaks of hydrotalcite at (0 0 2), (0 13), (–113) and (–311) (JCPDS 78-1219), indicating the typical hydrotalcite structure [20]. And the characteristic peak (001) represented calcium hydroxide (JCPDS 44-1481). It is proved that the precipitate is a mixture with CaAl-LDH-Cl as the main component. The d spacing value (d_{002}) of pristine waste-CaAl-LDH-Cl was calculated to be 7.853 Å by Jade 6.5.

The FTIR spectrums of waste-CaAl-LDH-Cl are presented in Fig. 2c. The information of wavenumber and the corresponding functional group is shown in the figure [20,21]. The result illustrated that the FTIR spectrum of the waste-CaAl-LDH-Cl was a typical spectrum of layered double hydroxides [22]. It should be noticed that the waste-CaAl-LDH-Cl had a weak characteristic peak of SO_4^{2-} at 1,118 cm^{-1} [23], which was due to the incomplete removal of SO_4^{2-} in the DCW in the first stage by the ultra-high lime with the aluminum process.

The SEM of waste-CaAl-LDH-Cl is shown in Fig. 2d. The waste-CaAl-LDH-Cl microphotography revealed that was a layered crystal with a smooth surface, which was consistent with the typical layered double hydroxides [24,25].

3.2. Effect of contact time and CR initial concentration

Fig. 3 shows the effect of contact time and initial dye concentration of the CR uptake on the waste-CaAl-LDH-Cl at 303 K. It could be seen that the adsorption of CR is rapid at the initial stage of the contract period, but it gradually reached equilibrium after 60 min. This is due to the high

concentration of CR and more adsorption sites in the initial stage of adsorption, which leads to the high adsorption driving force and the rapid increase of adsorption capacity.

3.3. Effect of solution temperature on CR adsorption

Fig. 4 shows the effects of temperature on the CR adsorption uptake for various initial dye concentrations. The CR adsorption uptakes were found to increase with the increase in solution temperature from 303 to 313 K for all initial concentrations. The results indicated that the adsorption reaction of CR adsorbed by waste-CaAl-LDH-Cl is an endothermic process.

3.4. Effect of solution pH on CR adsorption

Fig. 5 shows the effect of solution pH on the CR removal at initial pH values of 4, 6, 10, 12 and original pH. As shown in Fig. 5, the acid condition was favorable for CR removal and the removal percentage was above 98%. This can be attributed to the surface of the CaAl-LDH-Cl is protonated and positively charged at acid conditions. The electrostatic attraction between the adsorbent and the anionic dye increases. When pH is not adjusted, the removal percentage of CR is 96.32%. At pH 10 and 12, the removal efficiency of CR decreased sharply, and the removal percentage of CR is 93.16% and 80.88%, separately. A similar observation was obtained by Fernando Pereira de Sá [26]. In addition, Fig. 5 shows that the waste-CaAl-LDH-Cl has a wide range of pH(4~10) adaptation as an adsorbent, which makes it have a wide range of application prospects. The pH of natural water or wastewater is usually around 6–9 [27], thus there is no need to adjust the solution pH in view of practical application. Therefore, there is no need to adjust pH in this experiment.

The results of the adsorption of CR onto the waste-CaAl-LDH-Cl under different initial pH conditions are reported in Table 3. It would appear that the concentration of Cl^- and Ca^{2+} in the effluent after adsorption treatment meet the requirements for the reuse of Cl^- (<250 mg/L) and Ca^{2+} (<180 mg/L) in the reuse of urban recycling water-water quality standard for industrial uses (GBT 19923-2005). The Ca^{2+} is more in acid condition, likely due to the reaction of $Ca(OH)_2$ of waste-CaAl-LDH-Cl and HNO_3 to release more Ca^{2+}.

3.5. Adsorption kinetics

By fitting the data of Fig. 3, the fitting plots of the pseudo-first-order kinetic model and pseudo-second-order kinetic model were obtained, as shown in Fig. 6, and the fitting data are shown in Table 4.

In this experiment, kinetic models including the pseudo-first-order equation [Eq. (3)] and pseudo-second-order equation [Eq. (4)] were mentioned [28].

$$\ln\left(q_e - q_t\right) = \ln q_{e,\mathrm{cal}} - k_1 t \tag{3}$$

$$\frac{t}{q_t} = \frac{1}{k_2 q_{e,\mathrm{cal}}^2} + \frac{t}{q_{e,\mathrm{cal}}} \tag{4}$$

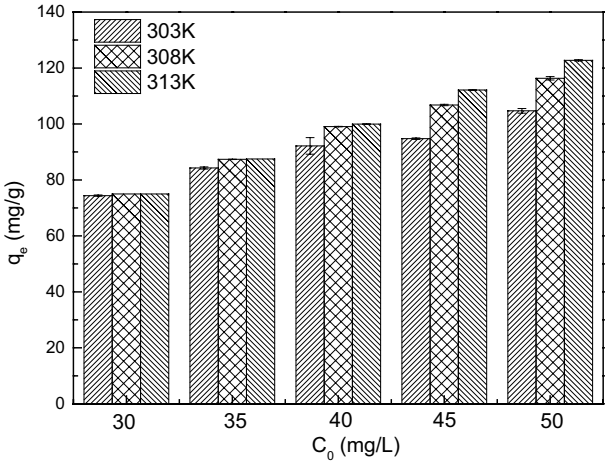

Fig. 4. Effect of solution temperature on CR uptake at various initial concentrations.

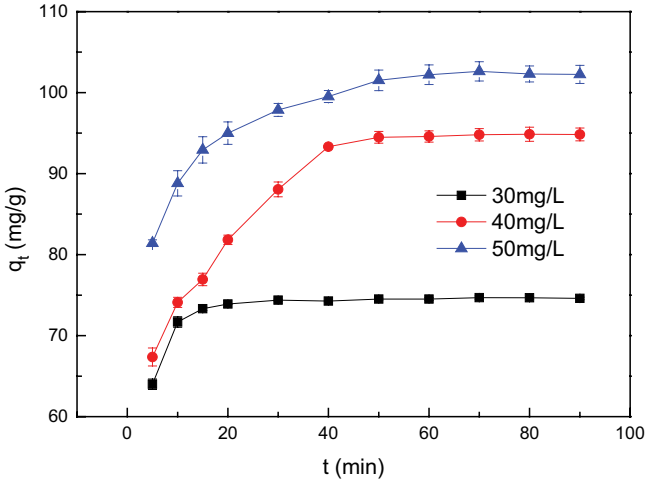

Fig. 3. Effect of contact time on CR adsorption on waste-CaAl-LDH-Cl at various initial concentrations.

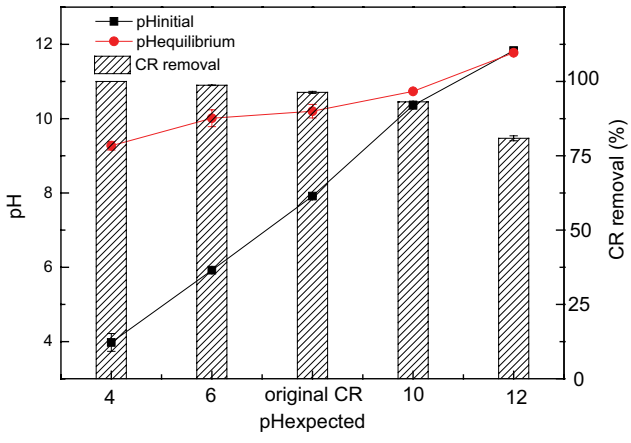

Fig. 5. Effect of solution pH on CR removal.

Table 3
Results of the adsorption of CR onto the LDH under different initial pH condition

$pH_{expected}$	$pH_{initial}$	$pH_{equilibrium}$	CR removal (%)	q_e	Cl^-	Ca^{2+}
4	3.97	9.27	100	125	36.66	35.27
6	5.92	10	98.72	123.4	43.33	29.39
$pH_{original}$	7.91	10.2	96.32	120.41	39.67	20.57
10	10.36	10.73	93.16	116.44	36.67	19.24
12	11.83	11.77	80.88	101.11	34	18.3

Table 4
Pseudo-first-order and pseudo-second-order kinetic model parameters for adsorption of CR

c_0 (mg/L)	$q_{e,exp}$ (mg/g)	Pseudo-first-order model				Pseudo-second-order model			
		$q_{e1,cal}$	k_1	R^2_{adj}	RMSE (%)	$q_{e2,cal}$	k_2	R^2_{adj}	RMSE (%)
30	74.693	5.226	0.065	0.8809	62.14	75.131	0.028	0.9999	0.22
40	94.858	73.943	0.099	0.9802	37.05	99.01	0.003	0.9993	0.77
50	102.425	30.578	0.07	0.9661	34.23	104.603	0.005	0.9999	0.24

Note: The $q_{e,exp}$ is experimental equilibrium adsorption capacity. The $q_{e,cal}$ is theoretical equilibrium adsorption capacity. The RMSE is the root mean squared error, which measured the differences of $q_{e,exp}$ and $q_{e,cal}$. The smaller the RMSE, the better the model fitting.

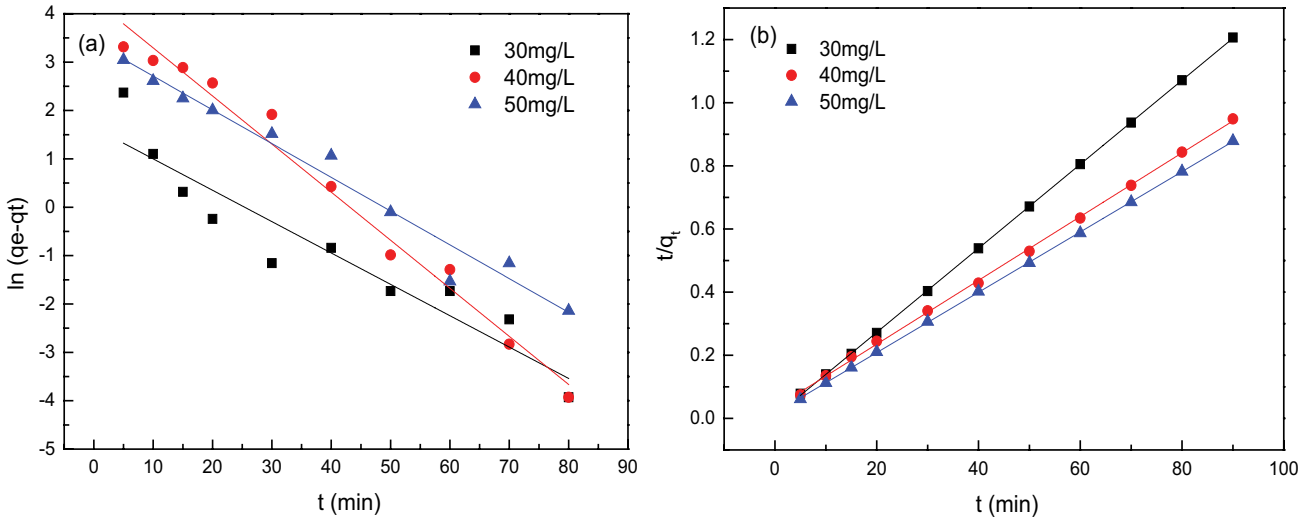

Fig. 6. Adsorption kinetic plots for the adsorption of CR on waste-CaAl-LDH-Cl: (a) pseudo-first-order model and (b) pseudo-second-order model. Conditions: *C*(CR) = 30, 40 and 50 mg/L, *m*(waste-CaAl-LDH-Cl) = 0.4 g/L, *V* = 100 mL, *t* = 90 min, *T* = 303 K, *r* = 200 rpm. pH was kept original.

where q_e and q_t are equilibrium adsorption capacity (mg/g) and adsorption capacity at a given time t, respectively. q_e can be obtained in Fig. 3, which is the adsorption capacity at t = 90 min. $q_{e,cal}$ denotes the calculated adsorption capacity (mg/g). k_1 and k_2 are the pseudo-first-order and pseudo-second-order rate constants, respectively. The linear plot of $\ln(q_e - q_t)$ vs. t gave a slope of k_1 and intercept of $\ln q_{e,cal}$ (Fig. 6a). The linear plot of t/q_t vs. t gave $1/q_{e,cal}$ as the slope and $1/(k_2 q^2_{e,cal})$ as the intercept (Fig. 6b).

According to Fig. 6 and Table 4, it could be seen that the kinetic data of CR adsorption by waste-CaAl-LDH-Cl had a better correlation with the pseudo-second-order model (R^2 > 0.999, Smaller RMSE). In addition, the $q_{e,cal}$ values calculated by the pseudo-second-order model were very close to the experimental values $q_{e,exp}$. Therefore, the adsorption of CR on waste-CaAl-LDH-Cl fitted well to the pseudo-second-order model. As shown in Table 4, the second-order rate constant changes almost an order of magnitude when the initial concentration changes from 30 to 40 mg/L. This illustrated that the adsorption reaction rate at 30 mg/L was faster than that at 40 mg/L, which was consistent with the adsorption equilibrium time in Fig. 3.

This kind of phenomenon of data also appears in the research of Ahmad & Rahman [29] and Hameed et al. [30].

3.6. Diffusion mechanism

The kinetic results were further analyzed by using the intraparticle diffusion model by using the following equation [29].

$$q_t = k_{pi} t^{1/2} + c_i \tag{5}$$

where k_{pi} is the rate constant of stage i, is obtained from the slope of the straight line of q_t vs. $t^{1/2}$. c_i is the intercept, which represents the influence of the interface layer. The rate-limiting process is only due to the intraparticle diffusion if the plot passes through the origin. Otherwise, some other mechanism along with intraparticle diffusion is also involved

According to Fig. 7 and Table 5, it could be seen that the intraparticle diffusion line was divided into two segments without passing the origin over the all-time range. The results indicate that more than one process affected the adsorption [30].

3.7. Adsorption isotherms

Langmuir and Freundlich's models were used to describe adsorption isotherms. The linear form of Langmuir and Freundlich isotherm equations are given as Eqs. (6) and (7), respectively [31].

$$\frac{c_e}{q_e} = \frac{c_e}{q_m} + \frac{1}{q_m K_L} \tag{6}$$

where c_e (mg/L) is the equilibrium concentration of the CR. q_m and q_e (mg/g) are the maximum adsorption capacity and equilibrium adsorption capacity, respectively; K_L is the Langmuir constant; A straight line with slope of $1/q_m$ and intercept of $1/(q_m K_L)$ was obtained when c_e/q_e is plotted against c_e (Fig. 8a).

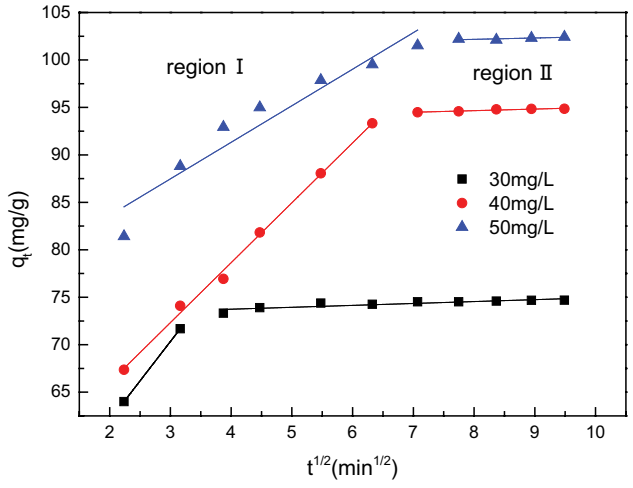

Fig. 7. The plot of the intraparticle diffusion model for the adsorption of CR on waste-CaAl-LDH-Cl.

$$\ln q_e = \ln K_F + \frac{1}{n} \ln c_e \tag{7}$$

where K_F is the Freundlich constant; n is the Freundlich adsorption index. The plot of $\ln q_e$ vs. $\ln c_e$ gave a straight line with a slope of $1/n$ and an intercept of $\ln K_F$ (Fig. 8b). $n > 1$ indicates that the adsorbate is favorable for adsorption on the adsorbent, and the adsorption is a physical process, while $n < 1$ illustrates that the adsorption is a chemical process [31].

Fig. 8a and b present plots of adsorption linearized isotherms of the Langmuir and Freundlich model, respectively. Table 6 is the linearized isotherm parameters at different temperatures. Fig. 8a and Table 6 show a good agreement between the experimental and the calculated q_m values, all the R^2 values obtained from the Langmuir model were higher ($R^2 > 0.98$) and all RMSE values were smaller, indicating that the adsorption of CR on waste-CaAl-LDH-Cl fitted well to Langmuir model. Therefore, the maximum adsorption capacity of CR on waste-CaAl-LDH-Cl is 123.9 mg/g at 313 K. Tables 7 and 8 show the adsorption capacities of reported other adsorbents made from waste and layered double hydroxide materials for CR, respectively. As shown in Tables 7 and 8, 123.9 mg/g is at the medium level, generally higher than the unmodified adsorbent and lower than the modified adsorbent. It is concluded that the waste-CaAl-LDH-Cl is an easily available and effective adsorbent.

3.8. Thermodynamic analyses

Thermodynamic parameters provide in-depth information about adsorption including energy change and reaction type. Therefore, standard free energy ($\Delta G°$), standard enthalpy($\Delta H°$) and standard entropy ($\Delta S°$) were calculated and analyzed. The value of $\Delta G°$, $\Delta H°$ and $\Delta S°$ could be obtained from the following equation [29,43,44]:

$$\Delta G° = -RT \ln k_L \tag{8}$$

Table 5
Intraparticle diffusion model constants for adsorption of CR

Model	Constants	c_0 (mg/L)		
		30	40	50
Intraparticle diffusion model	k_{p1}	8.297	6.312	3.851
	k_{p2}	0.201	0.168	0.143
	c_1	45.449	53.395	75.921
	c_2	72.935	93.316	101.020
	R_1^2	–	0.9959	0.9087
	R_2^2	0.7607	0.8750	0.4496
	$RMSE_1$ (%)	–	60.32	209.78
	$RMSE_2$ (%)	21.87	5.95	9.99

Note: k_{p1}, c_1, R_1^2 and $RMSE_1$ are the parameters of region I. k_{p2}, c_2, R_2^2 and $RMSE_2$ are the parameters of region II.

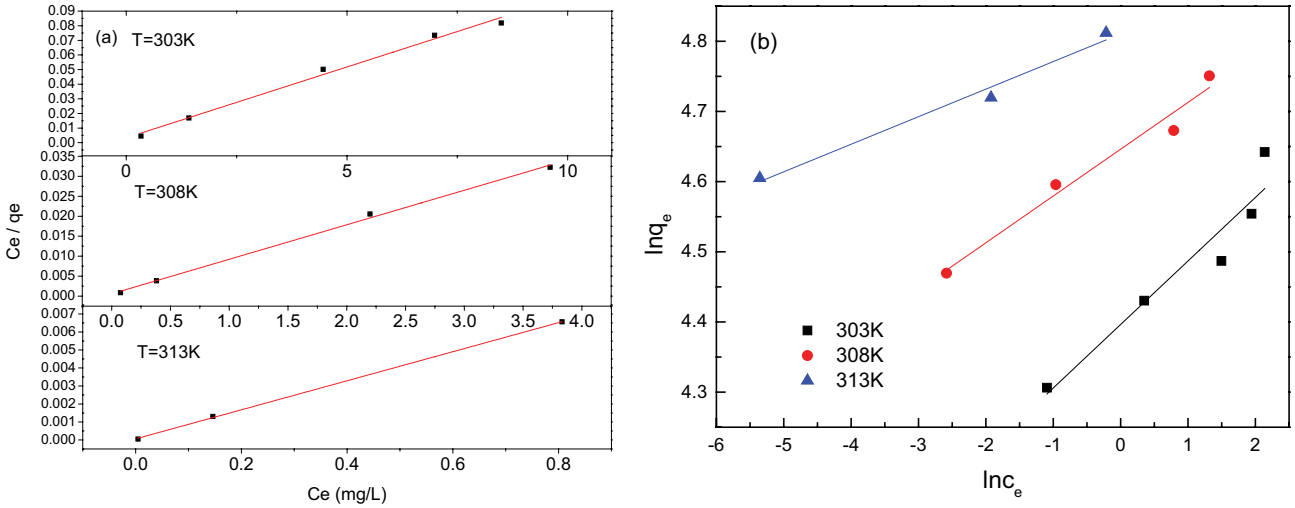

Fig. 8. The plot of Langmuir linearized isotherm (a) and plot of Freundlich linearized isotherm (b). Conditions: *C*(CR) = 30, 35, 40, 45 and 50 mg/L, *m*(waste-CaAl-LDH-Cl) = 0.4 g/L, *V* = 100 mL, *t* = 90 min, *T* = 303, 308, and 313 K, *r* = 200 rpm. The pH did not change.

Table 6
Linearized isotherm parameters of Langmuir and Freundlich model for adsorption of CR on waste-CaAl-LDH-Cl

		Langmuir				Freundlich			
Temperature (K)	$q_{m,exp}$ (mg/g)	q_m	k_L	R^2	RMSE (%)	K_F	n	R^2	RMSE (%)
303	103.76	103.1992	2.8925	0.9890	0.356	81.1582	11.0473	0.8937	4.137
308	115.67	115.7407	14.6615	0.9968	0.0834	104.1883	14.9948	0.9599	2.399
313	122.98	123.9157	132.2192	0.9994	0.0082	122.7758	25.4647	0.9667	1.892

Note: The $q_{m,exp}$ is the experimental maximum adsorption capacity. The RMSE is the root mean squared error, which measured the differences of $q_{e,exp}$ and $q_{e,cal}$. The smaller the RMSE, the better the model fitting.

Table 7
Adsorption capacities of CR on the waste-CaAl-LDH-Cl and other adsorbents made form waste

Adsorbent	q_{max} (mg/g)	References
Wheat bran/rice bran	22.73/14.63	[32]
Ball-milled sugarcane bagasse	38.2	[33]
Waste-CaAl-LDH-Cl	123.9	This study
Hydrogel made from bleached pineapple peel	138.89	[34]
Tomato processing waste-AC	435	[35]
Coir pith-AC	500	[36]

Note: AC is activated carbon.

$$\ln k_L = \frac{\Delta S^\circ}{R} - \frac{\Delta H^\circ}{RT} \quad (9)$$

where *R* (8.314 J/mol K) is the gas constant; *T* (K) is the absolute solution temperature and k_L (l/mg) is the Langmuir isotherm constant; The values of ΔH° and ΔS° can be calculated, respectively from the slope and intercept of $\ln k_L$ vs. $1/T$ plot (Fig. 9).

Table 8
Adsorption capacities of CR on the waste-CaAl-LDH-Cl and other layered double hydroxide materials

Adsorbent	q_{max} (mg/g)	References
CaAl-NO_3-LDH	59.416	[37]
CaAl-Cl-LDH	72.569	[38]
MgFe-CO_3-LDH	104.60	[39]
MgAl-Cl-LDH	111.11	[17]
Waste-CaAl-LDH-Cl	123.9	This study
NiFe-Cl-LDH	244.87	[16]
NiFe-LDH/NiFe-LDO	205/330	[40]
ZnAl-CO_3-LDH/ZnAl-CO_3-MW	210.08/462.96	[41]
Fe_3O_4@MgAl-LDH	813	[42]

Note: MW is microwave.

The calculated values of ΔG°, ΔH° and ΔS° for adsorption of CR on waste-CaAl-LDH-Cl are shown in Table 9. At all temperatures, ΔG° values were negative and decreased as temperature increased, indicating that the adsorption of CR on waste-CaAl-LDH-Cl was spontaneous and the higher temperature was favorable to

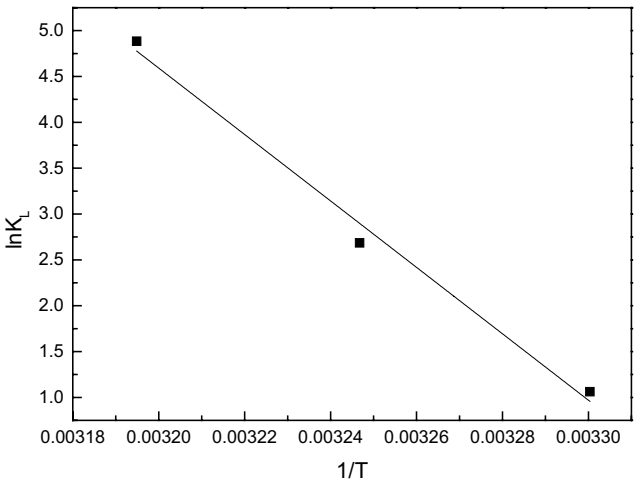

Fig. 9. Thermodynamic plot for adsorption of CR on waste-CaAl-LDH-Cl.

the adsorption. The positive ΔH value indicated that the adsorption reaction was an endothermic process. Moreover, the positive $\Delta S°$ indicated the randomness at the solid-solution interface was increasing, which proved the affinity of the adsorbent for adsorbate was greater.

Physisorption and chemisorption can be classified according to $\Delta H°$. The energy ($\Delta H°$) for chemisorption ranges from 80 to 450 kJ/mol, whereas the $\Delta H°$ values for the physical forces are as follows: van der Waals forces (4–10 kJ/mol), H-bonding (2–40 kJ/mol) and electrostatic interactions (20–80 kJ/mol) [45]. Based on the above reports and the data of $\Delta H°$ = 301.1145 kJ/mol in Table 9, which indicated that the adsorption of CR on waste-CaAl-LDH-Cl was mainly the chemisorption process.

Generally, $\Delta G°$ values for chemisorption are in the range –20–0 kJ/mol, and those for physisorption range between –80 and –400 kJ/mol [27]. In this study, the $\Delta G°$ values for CR on all temperatures were in the range of –20–0 kJ/mol, revealing that adsorption was chemisorption.

3.9. Mechanisms of CR adsorption onto waste-CaAl-LDH-Cl

For further probe, the molecular interaction of CR with the adsorbents, XRD diffraction patterns, FTIR spectra and SEM morphologies of waste-CaAl-LDH-Cl before and after CR adsorption are compared in Fig. 10.

In Fig. 10a, the main characteristic peaks of the layered double hydroxides such as (002), (013), (–113) and (–311) gradually decreased and disappeared after adsorption 30 and 50 mg/L CR, and the d spacing value (d_{002}) of pristine waste-CaAl-LDH-Cl did not change, indicating that CR was adsorbed on the surface, but not intercalated into the middle layer of waste-CaAl-LDH-Cl by ion exchange. In addition, according to JCPDS Card No.05-0586, the peak at 29.400° (104) may be due to the existence of calcium carbonate in the solid waste precipitate. This is due to the ultra-high lime aluminum process will absorb carbon dioxide in the air to generate calcium carbonate during operation. And because CR is amorphous, it does not show narrow peaks.

Table 9
Thermodynamic parameters for adsorption of CR on waste-CaAl-LDH-Cl

T (K)	$\Delta G°$ (kJ/mol)	$\Delta H°$ (kJ/mol)	$\Delta S°$ (kJ/mol K)	R^2
303	–2.6757			
308	–6.8761	301.1145	1.0017	0.98156
313	–12.7107			

Therefore, the strongest crystallinity of the adsorbed sample may be calcium carbonate which does not participate in the adsorption reaction.

The FTIR spectra of CR, waste-CaAl-LDH-Cl, and waste-CaAl-LDH-Cl after adsorption 30 and 50 mg/L CR are also performed and depict in Fig. 10b. For CR, the characteristic peaks at 3,467; 1,581; 1,064 and 1,176 cm^{-1} were identified as $–NH_2$ stretching vibration, aromatic skeletal vibration, S=O symmetric and asymmetric stretch bond, respectively [46,47]. After CR adsorption, the appearance of two new bands at 1,176/1,172 cm^{-1} and 1,045 cm^{-1} further confirmed the adsorption of CR. The shift of characteristic peaks to low frequency also confirmed the existence of electrostatic interaction or hydrogen bond [27]. The main layer of LDH ($[Ca_2Al(OH)_6]^+$) is positively charged and CR (CR-SO_3^-) in aqueous solution is negatively charged, so there is an electrostatic attraction between waste-CaAl-LDH-Cl and CR (CR-SO_3^- + $[Ca_2Al(OH)_6]^+ \rightarrow$ CR-SO_3^- ~ $^+[Ca_2Al(OH)_6]$). Moreover, the adsorption of CR may be also due to the hydrogen bond formed between the electronegative atoms of dye and adsorbents such as oxygen, nitrogen or sulfur and hydrogen atoms [48]. In Fig. 10b, it was evident that the –OH (3,488 cm^{-1}) in waste-CaAl-LDH-Cl slightly shifted to lower wavenumber (3,436 cm^{-1}) after CR adsorption, reflecting the possibility of hydroxyl groups participating in the adsorption process through a hydrogen bond. Furthermore, CR may be adsorbed on the surface of waste-CaAl-LDH-Cl due to a coordination effect of metal ions (Ca^{2+} and Al^{3+}) with $–NH_2$ and $–SO_3^-$ groups of CR [48,49]. As Fig. 9b shows, the peaks at 532 and 424 cm^{-1} indicated the lattice vibrations of Al–OH and Ca–OH, which disappeared completely after adsorption CR of 50 mg/L.

The SEM morphologies of waste-CaAl-LDH-Cl after adsorption 30 and 50 mg/L CR are shown in Fig. 10c and d. Fig. 10c shows that after adsorbing 30 mg/L CR, the adsorbent presented a relatively broken shape, with small particles on the surface. This is consistent with the research conclusion of Fernando Pereira de Sá [26]. After adsorbing 50 mg/L CR, as shown in Fig. 10d, the layered structure was almost invisible and completely wrapped by granular materials. The electron microscope images further proved that the adsorption was surface adsorption.

The above analysis showed that the adsorption between the waste-CaAl-LDH-Cl and CR was mainly surface adsorption. The mechanism may be electrostatic interaction between the positively charged adsorbent surface and negatively charged SO_3^- groups of CR, the hydrogen bond between $–NH_2$ of CR and –OH of the adsorbent surface and the chemical complexation between M (metal

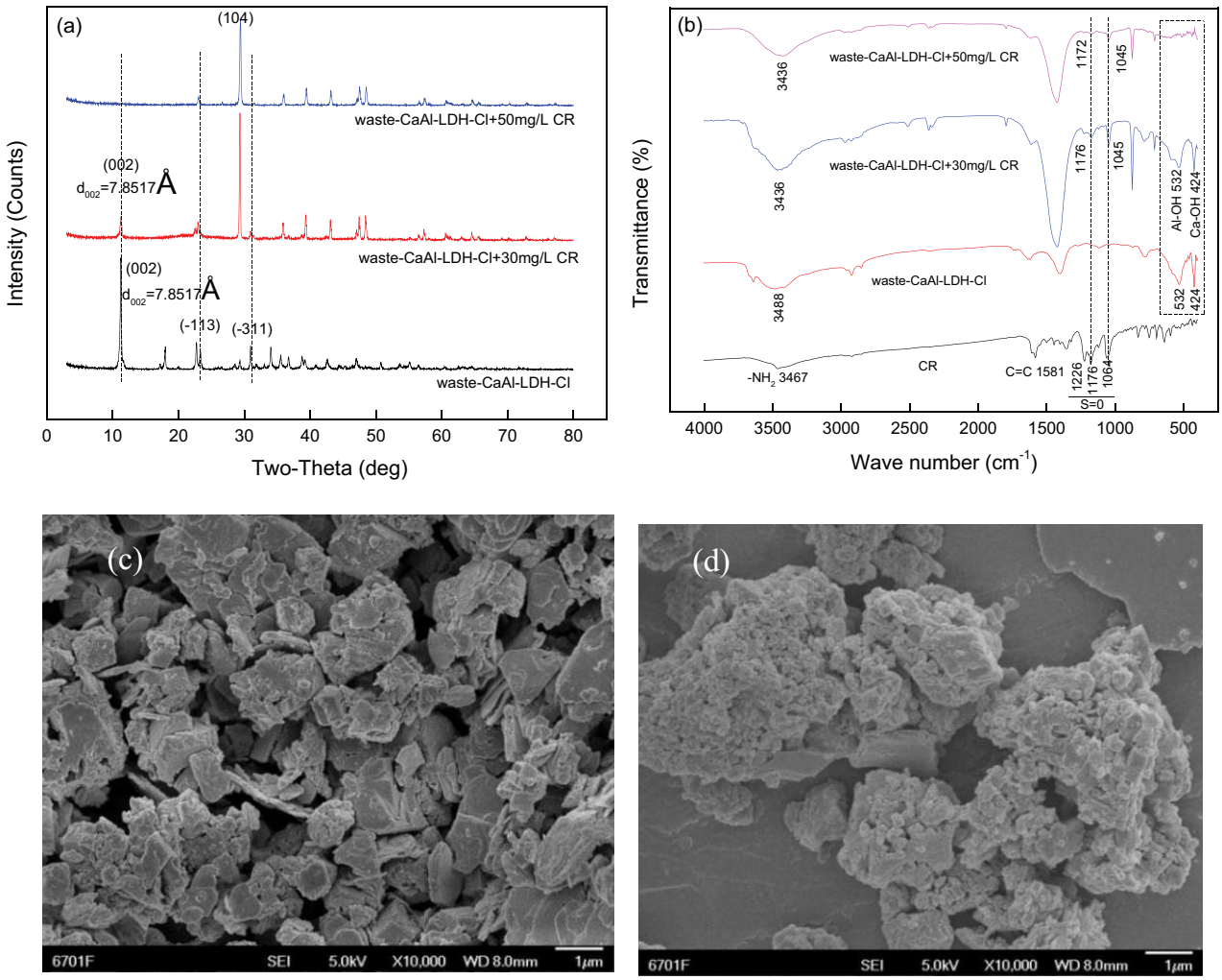

Fig. 10. (a) XRD patterns, (b) FTIR spectrums and (c & d) SEM morphologies of waste-CaAl-LDH-Cl before and after CR adsorption.

Fig. 11. The process and mechanism diagram of the experiment.

ion) and sulfonate groups of CR. The experimental process and mechanism are shown in Fig. 11.

4. Conclusions

This study showed that waste-CaAl-LDH-Cl is an effective adsorbent for the removal of CR dye from the aqueous solutions. Adsorption of CR was found to increase with the increase in contact time, initial dye concentration and solution temperature. The adsorption of CR on waste-CaAl-LDH-Cl was favored at an acidic medium. The adsorption kinetics followed the pseudo-second-order model, whereas Langmuir adsorption isotherm fitted better to obtained data. The highest adsorption of 123.9 mg/g was recorded at 90 min and 313 K. The intraparticle diffusion indicates that more than one process affected the adsorption. The values of $\Delta G°$, $\Delta H°$ and $\Delta S°$ were –2.6757 ~ –12.7107 kJ/mol, 301.1145 kJ/mol and 1.0017 kJ/mol K, respectively, indicating that the adsorption process was spontaneous and endothermic chemisorption. And the randomness at the solid-solution interface was increasing. Further, the FTIR, XRD and SEM analysis, results showed that the adsorption mechanism also included the electrostatic interaction, hydrogen bond and chemical complexation. These results showed that waste-CaAl-LDH-Cl obtained from the treatment of DCW using ultra-high lime with the aluminum process can be used as an adsorbent to effectively remove anionic organic pollutants in dye wastewater, so as to achieve the purpose of resource recycling and utilization.

Acknowledgments

This study was financially supported by the National Natural Science Foundation of China (grant number 51268034). The authors would like to thank the anonymous reviewers for making useful suggestions.

References

[1] L.-B. Niu, K. Nakada, Effect of chloride and sulfate ions in simulated boiler water on pitting corrosion behavior of 13Cr steel, Corros. Sci., 96 (2015) 171–177.
[2] H.-Y. Yu, S.-J. Shi, R. Xu, J. Zhao, Study on the removal mechanism of chemically bonded chloride ions in concrete under electric field, Ferroelectrics, 549 (2019) 126–136.
[3] P. Fang, Z.-j. Tang, X.-b. Chen, J.-h. Huang, Z.-x. Tang, C.-p. Cen, Chloride ion removal from the wet flue gas desulfurization and denitrification wastewater using Friedel's salt precipitation method, J. Chem., 2018 (2018) 5461060, doi: 10.1155/2018/5461060.
[4] A. Abdel-Wahab, B. Batchelor, Chloride removal from recycled cooling water using ultra-high lime with aluminum process, Water Environ. Res., 74 (2002) 256–263.
[5] L. Lv, P.D. Sun, Z.Y. Gu, H.G. Du, X.J. Pang, X.H. Tao, R.F. Xu, L.L. Xu, Removal of chloride ion from aqueous solution by ZnAl-NO_3 layered double hydroxides as anion-exchanger, J. Hazard. Mater., 161 (2009) 1444–1449.
[6] H.H. Chen, L.R. Yuan, M.X. Li, L. Hang, W.J. Wei, Research progress in technology of chloride removal from aqueous solution, in China, J. Mater. Prot., 48 (2015) 31–35.
[7] M. Carmona, A. Pérez, A.D. Lucas, L. Rodríguez, J.F. Rodriguez, Removal of chloride ions from an industrial polyethylenimine flocculant shifting it into an adhesive promoter using the anion exchange resin amberlite IRA-420, React. Funct. Polym., 68 (2008) 1218–1224.
[8] A. Chmielarz, W. Gnot, Conversion of zinc chloride to zinc sulphate by electrodialysis – a new concept for solving the chloride ion problem in zinc hydrometallurgy, Hydrometallurgy, 61 (2001) 21–43.
[9] X.L. Wu, Z.Q. Liu, X. Liu, Chloride ion removal from zinc sulfate aqueous solution by electrochemical method, Hydrometallurgy, 134–135 (2013) 62–65.
[10] F. Feki, F. Aloui, M. Feki, S. Sayadi, Electrochemical oxidation post-treatment of landfill leachates treated with membrane bioreactor, Chemosphere, 75 (2009) 256–260.
[11] A. Abdel-Wahab, B. Batchelor, J. Schwantes, An equilibrium model for chloride removal from recycled cooling water using the ultra-high lime with aluminum process, Proc. Water Environ. Fed., 2002 (2002) 23–39.
[12] L.P. Wang, W.H. Lee, S.M. Tseng, T.W. Cheng, Removal of chloride ions from an aqueous solution containing a high chloride concentration through the chemical precipitation of Friedel's salt, Mater. Trans., 59 (2018) 297–302.
[13] A. Abdel-Wahab, B. Batchelor, Effects of pH, temperature, and water quality on chloride removal with ultra-high lime with aluminum process, Water Environ. Res., 78 (2006) 930–937.
[14] J.O. Eniola, R. Kumar, A.A. Al-Rashdi, M.O. Ansari, M.H. Barakat, Fabrication of novel $Al(OH)_3$/CuMnAl- layered double hydroxide for detoxification of organic contaminants from aqueous solution, ACS Omega,4 (2019) 18268–18278.
[15] N. Almoisheer, F.A. Alseroury, R. Kumar, M. Aslam, M.A. Barakat, Adsorption and anion exchange insight of indigo carmine onto CuAl-LDH/SWCNTs nanocomposite: kinetic, thermodynamic and isotherm analysis, RSC Adv., 9 (2019) 560–568.
[16] T.U.T. Dao, K.H. Nguyen, T.T. Nguyen, H.T.T. Nguyen, D.T. Sy, T.D. Nguyen, A.T. Nguyen, Process optimization studies of Congo red dye adsorption onto nickel iron layered double hydroxide using response surface methodology, Solid State Phenom., 298 (2019) 83–88.
[17] R. Lafi, K. Charradi, M.A. Djebbi, A. Ben Haj Amara, A. Hafiane, Adsorption study of Congo red dye from aqueous solution to Mg–Al–layered double hydroxide, Adv. Powder Technol. Jpn., 27 (2016) 232–237.
[18] E.T. Tolonen, T. Hu, J. Rämö, U. Lassi, The removal of sulphate from mine water by precipitation as ettringite and the utilisation of the precipitate as a sorbent for arsenate removal, J. Environ. Manage., 181 (2016) 856–862.
[19] R.-J. Wu, J.-C. Liu, Removal of phosphate using ettringite synthesized from industrial by-products, Water Air Soil Pollut., 229 (2018) 1–14.
[20] D. Li, X.Y. Guo, Q.H. Tian, Z.P. Xu, R.Z. Xu, L. Zhang, Synthesis and application of Friedel's salt in arsenic removal from caustic solution, Chem. Eng. J., 323 (2017) 304–311.
[21] X.J. Sui, Synthesis of Ettringites Using Large-Volume Industrial Wastes and Their Applications in Solidification/Stabilization of Metal Pollutants (Monex Fly Ash), Faculty of the College of Graduate Studies Lamar University, 1996, pp. 40–49.
[22] Y.C. Dai, G.R. Qian, Y.L. Cao, Y. Chi, Y.F. Xu, J.Z. Zhou, Q. Liu, Z.P. Xu, S.Z. Qiao, Effective removal and fixation of Cr(VI) from aqueous solution with Friedel's salt, J. Hazard. Mater., 170 (2009) 1086–1092.
[23] E. Ciliberto, S. Ioppolo, F. Manuella, Ettringite and thaumasite: a chemical route for their removal from cementious artefacts, J. Cult. Heritage, 9 (2008) 30–37.
[24] S. Jamil, A.R. Alvi, S.R. Khan, Layered double hydroxides (LDHs): synthesis & applications LDG, Prog. Chem., 31 (2019) 394–412.
[25] J.Y. Ma, Z.B. Li, Preparation of Ca-Al Hydrotalcite-Like Compounds and Their Desilication in Sodium Aluminate Solution, China, Science, China Press, 40 (2009) 577–584.
[26] F.P. de Sá, B.N. Cunha, L.M. Nunes, Effect of pH on the adsorption of sunset yellow FCF food dye into a layered double hydroxide (CaAl-LDH-NO_3), Chem. Eng. J., 215–216 (2013) 122–127.

[27] L. Deng, H. Zeng, Z. Shi, W. Zhang, J. Luo, Sodium dodecyl sulfate intercalated and acrylamide anchored layered double hydroxides: a multifunctional adsorbent for highly efficient removal of Congo red, J. Colloid Interface Sci., 521 (2018) 172–182.
[28] R. Kumar, S.A. Ansari, M.A. Barakat, A. Aljaafari, M.H. Cho. A polyaniline@MoS_2-based organic–inorganic nanohybrid for the removal of Congo red: adsorption kinetic, thermodynamic and isotherm studies, New J. Chem., 42 (2018) 18802–18809.
[29] M.A. Ahmad, N.K. Rahman, Equilibrium, kinetics and thermodynamic of Remazol brilliant orange 3R dye adsorption on coffee husk-based activated carbon, Chem. Eng. J., 170 (2011) 154–161.
[30] B.H. Hameed, A.A. Ahmad, N. Aziz, Adsorption of reactive dye on palm-oil industry waste: equilibrium, kinetic and thermodynamic studies, Desalination, 247 (2009) 551–560.
[31] R. Miandad, R. Kumar, M.A. Barakat, C. Basheer, A.S. Aburiazaiza, A.S. Nizami, M. Rehan, Untapped conversion of plastic waste char into carbon-metal LDOs for the adsorption of Congo red, J. Colloid Interface Sci., 511 (2018) 402–410.
[32] X.S. Wang, J.P. Chen, Biosorption of Congo red from aqueous solution using wheat bran and rice bran: batch studies, Sep. Sci. Technol., 44 (2009) 1452–1466.
[33] Z. Zhang, L. Moghaddam, I.M. O'Hara, W.O.S. Doherty, Congo red adsorption by ball-milled sugarcane bagasse, Chem. Eng. J., 178 (2011) 122–128.
[34] H. Dai, Y. Huang, H. Zhang, L. Ma, H. Huang, J. Wu, Y. Zhang, Direct fabrication of hierarchically processed pineapple peel hydrogels for efficient Congo red adsorption, Carbohydr. Polym., 230 (2020) 115599–115599.
[35] H. Saygili, F. Guzel, Behavior of mesoporous activated carbon used as a remover in Congo red adsorption process, Water Sci. Technol., 1 (2018) 170–183.
[36] C. Namasivayam, D. Kavitha, Removal of Congo red from water by adsorption onto activated carbon prepared from coir pith, an agricultural solid waste, Dyes Pigm., 54 (2002) 47–58.
[37] H.T.N. Thi, D.C. Nguyen, T.T. Nguyen, V.T. Tran, H.V. Nguyen, L.G. Bach, D.V. N-Vo, D.H. Nguyen, D.V. Thuan, D.T. Sy, T.D. Nguyen, Congo red dye removal using Ca-Al layered double hydroxide: kinetics and equilibrium, Key Eng. Mater., 814 (2019) 463–468.
[38] T.U.T. Dao, K.H. Nguyen, T.T. Nguyen, H.T.T. Nguyen, D.T. Sy, T.D. Nguyen, A.T. Nguyen, Adsorption isotherms and kinetic models for Congo red adsorption on Ca-Al layer double hydroxide adsorbent, Solid State Phenom., 298 (2019) 128–132.
[39] I.M. Ahmed, M.S. Gasser, Adsorption study of anionic reactive dye from aqueous solution to Mg–Fe–CO_3 layered double hydroxide (LDH), Appl. Surf. Sci., 259 (2012) 650–656.
[40] C. Lei, M. Pi, P. Kuang, Y. Guo, F. Zhang, Organic dye removal from aqueous solutions by hierarchical calcined Ni-Fe layered double hydroxide: Isotherm, kinetic and mechanism studies, J. Colloid Interface Sci., 496 (2017) 158–166.
[41] S. Chilukoti, T. Thangavel, Enhanced adsorption of Congo red on microwave synthesized layered Zn-Al double hydroxides and its adsorption behaviour using mixture of dyes from aqueous solution, Inorg. Chem. Commun., 100 (2019) 107–117.
[42] L. Lu, J. Li, D.H.L. Ng, P. Yang, P. Song, M. Zuo, Synthesis of novel hierarchically porous Fe_3O_4@MgAl- LDH magnetic microspheres and its superb adsorption properties of dye from water, J. Ind. Eng. Chem., 46 (2017) 315–323.
[43] F.M. Machado, C.P. Bergmann, T.H.M. Fernandes, E.C. Lima, B. Royer, T. Calvete, S.B. Fagan, Adsorption of reactive red M-2BE dye from water solutions by multi-walled carbon nanotubes and activated carbon, J. Hazard. Mater., 192 (2011) 1122–1131.
[44] L.D.T. Prola, F.M. Machado, C.P. Bergmann, F.E. de Souza, C.R. Gally, E.C. Lima, M.A. Adebayo, S.L.P. Dias, T. Calvete, Adsorption of direct blue 53 dye from aqueous solutions by multi-walled carbon nanotubes and activated carbon, J. Environ. Manage., 130 (2013) 166–175.
[45] M.O. Ansari, R. Kumar, S.A. Ansari, S.P. Ansari, M.A. Barakat, A. Alshahrie, M.H. Cho, Anion selective pTSA doped polyaniline@graphene oxide-multiwalled carbon nanotube composite for Cr(VI) and Congo red adsorption, J. Colloid Interface Sci., 496 (2017) 407–415.
[46] P. Zhang, G.R. Qian, H.F. Cheng, J. Yang, H.S. Shi, R.L. Frost, Near-infrared and mid-infrared investigations of na-dodecylbenzenesulfate intercalated into hydrocalumite chloride (CaAl-LDH-Cl), Spectrochim. Acta, Part A, 79 (2011) 548–553.
[47] M.H. Zhu, P. Hu, Instrumental Analysis, Higher Education Press, Beijing, China, 2008.
[48] R. Kumar, J. Rashid, M.A. Barakat, Synthesis and characterization of a starch/AlOOH/FeS_2 nanocomposite for the adsorption of Congo red dye from aqueous solution, RSC Adv., 4 (2014) 38334–38340.
[49] W. Yao, S.J. Yu, J. Wang, Y.D. Zou, S.S. Lu, Y.J. Ai, Enhanced removal of methyl orange on calcined glycerol-modified nanocrystallined Mg/Al layered double hydroxides, Chem. Eng. J., 307 (2017) 476–486.